Journal of Photochemistry, 6 (1976/77) 111 - 126

PHOTO-OXIDATION OF CH_3CHO VAPOR AT 3130 Å

JAMES WEAVER*, JAMES MEAGHER** and JULIAN HEICKLEN

Department of Chemistry and Center for Air Environment Studies, The Pennsylvania State University, University Park, Pa. 16802 (U.S.A.)

(Received March 1, 1976; revised June 14, 1976)

Summary

The photolysis of CH_3CHO vapor with radiation at 3130 Å in the presence of O_2 or O_2–N_2 mixtures was studied at 25 °C. Absolute quantum yields were obtained for the products CO, CO_2, CH_3OH, and CH_3CO_3H (peracetic acid). From them and the results of Archer *et al.*, it could be deduced that CH_3 + HCO are produced directly on absorption 5% of the time. An intermediate (I) which is a complex between triplet CH_3CHO and O_2 is produced 65% of the time, and it decomposes via:

$$I \rightarrow CH_3 + CO + HO_2 \quad (6)$$

$$I + M \rightarrow A + O_2 + M \quad (7)$$

with k_6/k_7 = 186 Torr for N_2 as a chaperone in reaction (7). O_2 is much less efficient than N_2 as a quenching agent for I, the best fit of the data occurring for an O_2 efficiency 20% that of N_2. For one atmosphere of air, the photon efficiency at 3130 Å to produce CO through I is 0.15. Under atmospheric conditions for an overhead sun the rate coefficients averaged over all wavelengths are 2.8×10^{-6} and 8.7×10^{-6} s^{-1}, respectively, for the production of HCO and HO_2 in the primary process, which gives the overall rate coefficient for free radical production to be 2.3×10^{-5} s^{-1}.

Introduction

The photochemical oxidation of aliphatic aldehydes has been shown to be an important process in the chemistry of photochemical smog [1]. In fact, the photo-oxidation of formaldehyde, acetaldehyde and propionaldehyde in the presence of nitrogen oxides produces the same products and biological effects as do hydrocarbon oxidations [1, 2]. Thus, understanding the mechanism of the photo-oxidation process for aldehydes is an important aspect of photochemical smog research.

*Present address: Eastman Kodak Co. Research Laboratories, Rochester, N.Y. (U.S.A.)

**Present address: Tennessee Valley Authority, Air Quality Branch, Muscle Shoals, Alabama (U.S.A.)

The first room temperature study of the photo-oxidation of acetaldehyde in both the vapor and liquid phases as well as in solution was made by Bowen and Tietz [3]. They found the major products of the reaction to be peroxides formed in a long chain. Studies on the photo-oxidation of both formaldehyde and acetaldehyde by Carruthers and Norrish [4] produced results that were, except for chain length, consistent with those of Bowen and Tietz. In 1941, work by Mignolet [5] further substantiated the results of these studies. McDowell and coworkers [6 - 8] in 1958 confirmed the presence of peracetic acid as a product in the photo-oxidation of acetaldehyde and also proposed diacetylperoxide, $CH_3C(O)-O-O-(O)CCH_3$, which was found in small amounts [8], as the product of the chain-terminating step. However, in a study by Calvert and Hanst [9] of acetaldehyde photo-oxidation at lower pressures (~42 Torr of CH_3CHO) no diacetylperoxide was obtained, although peracetic acid was again confirmed as a product. In 1964, Johnston and Heicklen [10] studied acetaldehyde photo-oxidation at even lower pressures ($[CH_3CHO]$ = 0.14 - 18 Torr, $[O_2]$ = 1.0 - 9.2 Torr) using mass spectral techniques. As principal products they reported CH_3OH and presumably CO and CO_2. Other products were H_2O, CH_2O, HCOOH, CH_3OOH, CH_3CO_2H, CH_3OOCH_3 and probably CH_3CO_3H. They also looked for, but could not find, diacetylperoxide as a product. However, they were unable to deduce a mechanism from their product analysis.

Since the photo-oxidation of acetaldehyde is complicated by the possible existence of long-lived excited states and by the number of different primary photolytic processes, work has also been done on the autoxidation of acetaldehyde in both the gas phase, in our laboratory [11], and in the liquid phase, by Clinton *et al.* [12]. In both of these studies neither CO nor diacetyl peroxide was detected, and the self-annihilation of the acetylperoxy radicals, CH_3CO_3, was shown to lead to methyl radicals, carbon dioxide and oxygen. In our gas phase work [11], the experimental results were consistent with a mechanism in which the acetyl radical, CH_3CO, oxidizes entirely by the addition reaction with O_2 to form the acetyl peroxy radical. Also, the main termination reactions were shown to be those involving the self-annihilation of the methylperoxy radicals (CH_3O_2).

On the basis of these past studies on the autoxidation of acetaldehyde, this work was undertaken to investigate the role of excited states and the photolytic primary processes in the photo-oxidation of acetaldehyde.

Experimental

Experiments were performed in a 100 cm^3 quartz infra-red gas cell with sodium chloride windows. Reaction mixtures were photolyzed through the windows with radiation at 3130 Å using an Illumination Industries Inc. medium pressure mercury arc lamp, type III 202, fitted with an appropriate filtering system. The filter system consisted of two Corning glass filters,

0-53 and 7-54, and a chemical filter of 1.25×10^{-4} *M* aqueous K_2CrO_4 solution in a 5 cm path length quartz cell. A conventional high vacuum line equipped with Vitron "O" rings was used for gas handling.

Photolysis was interrupted at various time intervals during an experiment to allow for infra-red analysis of two of the reaction products, methanol and peracetic acid, using a Beckman IR-10 infra-red spectrophotometer. Peracetic acid calibrations were performed by allowing the peracetic acid in some of the experiments to convert to acetic acid in the infra-red gas cell [13]. Thus, by measuring the acetic acid it was possible to deduce the amount of peracetic acid produced. Calibrations for methanol and acetic acid were performed using standard samples with consideration given to the acetic acid dimer–monomer equilibrium (K_p = 0.577 Torr at 25 °C) [14].

After the irradiation was completed, carbon dioxide and carbon monoxide were analyzed on a Gow-Mac gas chromatograph employing a thermistor detector at 0 °C. The CO_2 was separated from other reaction components on an 11 ft. × 1/4 in. o.d. copper column packed with Porapak QS and operated at room temperature with a helium carrier gas flow rate of 45.5 cm^3/min. The CO was separated from the other reaction components on an 8 ft. × 1/4 in. o.d. copper column packed with 13X molecular sieves operated at room temperature with a helium carrier gas flow rate of 50 cm^3/min. Both CO_2 and CO calibration were performed using standard samples.

The azomethane was prepared from a procedure by Renaud and Leitch [15]. It was purified by trap-to-trap distillation from —90 ° to —130 °C. The acetaldehyde, acetic acid and methanol were obtained from Fisher Scientific Company. The acetaldehyde was purified by distillation from —79 ° to —130 °C. Gas chromatographic analysis showed < 0.01% of any chemical impurity in either the purified acetaldehyde or azomethane. The O_2, N_2, CO_2, and CO were Matheson extra dry, prepurified, bone dry and chemically pure grades respectively.

The air was Matheson CO_2 free air which contained less than 5 p.p.m. CO_2. Before use, the azomethane and acetaldehyde were degassed at —130 ° and —196 °C respectively, and O_2, N_2 and air were passed over Drierite.

The production rates for peracetic acid and methanol were determined from the growth plots of the infra-red absorbances at 8.1 μm and 9.68 μm respectively. CO and CO_2 production rates were obtained by measuring the amount of CO and CO_2 in the reaction cell after photolysis. The absorbed light intensity was measured in separate actinometer experiments in which azomethane was photolyzed under the same experimental conditions but in the absence of acetaldehyde, O_2 and N_2. The pressure of azomethane used for the actinometry was determined by matching absorbances with the pressure of acetaldehyde used in an experimental run.

Results

The photolysis of acetaldehyde, with radiation at 3130 Å in the presence of air and oxygen–nitrogen mixtures was studied at 25 °C. The pressure

TABLE 1

Product quantum yields in the photolysis of acetaldehyde in the presence of O_2 and N_2 at 25 °C. $[CH_3CHO]/[O_2]$ study[a]

$\frac{[CH_3CHO]}{[O_2]}$	$[CH_3CHO]$ (Torr)	$[O_2]$ (Torr)	P_{total} (Torr)	$\Phi\{CO\}$	$\Phi\{CO_2\}$	$\Phi\{CH_3OH\}$	$\Phi\{CH_3CO_3H\}$
1.942	10.1	5.2	640	0.134 (0.153)	0.195 (0.251)	0.427 (0.351)	0.579 (0.520)
1.081	10.1	9.3	660	0.135 (0.150)	0.204 (0.227)	0.361 (0.322)	0.510 (0.490)
0.475	10.1	21.25	652	0.144 (0.153)	0.197 (0.184)	0.394 (0.273)	0.420 (0.428)
0.369	10.2	31.6	635	0.151 (0.157)	0.123 (0.162)	0.316 (0.246)	0.369 (0.393)
0.170	10.1	59.0	646	0.156 (0.159)	0.105 (0.122)	0.280 (0.196)	0.332 (0.319)
0.077	10.0	130	650	0.140 (0.170)	0.080 (0.082)	0.280 (0.145)	0.242 (0.231)
0.061	10.0	165	660	0.159 (0.174)	0.077 (0.073)	0.169 (0.132)	0.243 (0.208)
0.034	10.1	293	656	0.183 (0.202)	0.052 (0.057)	0.140 (0.116)	0.194 (0.165)
0.027	10.0	378	702	— (0.209)	— (0.050)	0.123 (0.108)	0.148 (0.146)
0.023	10.2	447	708	0.217 (0.226)	0.044 (0.048)	0.126 (0.109)	0.174 (0.140)
0.016	10.1	620	630	— (0.364)	— (0.048)	0.120 (0.145)	0.171 (0.124)

[a] $I_a = 6.25 \times 10^{-4}$ Torr/s. Values of quantum yields in parentheses are computed from the mechanism and the rate coefficient ratios listed in Table 5.

of acetaldehyde was varied from 3 to 30 Torr while the pressures of oxygen and nitrogen ranged from 5 to 620 Torr, and 0 to 680 Torr respectively.

Absolute quantum yields were obtained for the products CO, CO_2, methanol and peracetic acid. The quantum yields for methanol and peracetic acid were obtained by infra-red analysis while those for CO and CO_2 were obtained by gas chromatography. Although acetic acid is also a product of the reaction, infra-red analysis confirmed that all the acetic acid came from the decomposition of the peracetic acid. Also, we looked for but could find no evidence of CH_4, and thus this compound must have a quantum yield less than 0.01 in this system.

In Table 1 are given the product quantum yields for the case of constant acetaldehyde pressure, total pressure and absorbed light intensity with the oxygen pressure varying between 5 and 620 Torr. As was found in our previous work on the oxidation of acetyl radicals [11], the quantum yields of peracetic acid, CO_2 and methanol were observed to decrease as the ratio $[CH_3CHO]/[O_2]$ decreased. However, the quantum yield for CO did not exhibit this behavior and, in fact, had a slightly opposite dependence on this ratio. It should be noted that at values of $[CH_3CHO]/[O_2]$ less than about 0.03 the product quantum yields for CO_2, CH_3OH and CH_3CO_3H level off and become constant.

Table 2 contains the product quantum yields for experiments performed at constant acetaldehyde pressure, light intensity and O_2 pressure but with the total pressure varying between 20 and 660 Torr. Two sets of data are given: the first for a value of the $[CH_3CHO]/[O_2]$ ratio of 0.32 and the second for which this ratio is 1.0. For both data sets the quantum yields of CO, methanol and peracetic acid decrease as the total pressure increases. For the CO_2 quantum yields the trend is much less discernible and may be said to have little or no correlation with total pressure. A plot is shown in Fig. 1 of the reciprocal of the CO quantum yield against the effective total pressure [M] for both sets of data in Table 2. The major quenching gas is N_2, but we have defined $[M] = [O_2] + [N_2] + 3[CH_3CHO]$ in order to account for the more efficient quenching ability of acetaldehyde with respect to oxygen and nitrogen [16]. Later we will show that a best fit to the data in Table 1 is obtained by letting O_2 be only 0.20 as efficient as N_2. However, for the data in Fig. 1 the quenching by O_2 is negligible. The plot of Fig. 1 is a straight line accommodating the CO data at both $[CH_3CHO]/[O_2]$ ratios indicating that the reactions producing CO do not involve species also involved in the acetaldehyde–oxygen competition. The intercept of the plot is 1.5 and the half-quenching pressure is 188 Torr.

The product quantum yields for the case of constant acetaldehyde and air pressure, but with varying absorbed light intensity are given in Table 3. Figure 2 shows a log–log plot of the product quantum yields against the reciprocal of the absorbed light intensity. The data for peracetic acid can be fitted to a straight line of slope 1/2 indicating that $\Phi\{CH_3CO_3H\}$ is inversely proportional to $I_a^{1/2}$; a result also observed in the work on the oxidation of acetyl radicals [11]. The scatter in the data for the other product quantum

TABLE 2

Product quantum yields in the photolysis of acetaldehyde in the presence of O_2 and N_2 at 25 °C.
Total Pressure Study[a]

P_{total} (Torr)	$[CH_3CHO]$ (Torr)	$[O_2]$ (Torr)	$\frac{[CH_3CHO]}{[O_2]}$	$\Phi\{CO\}$	$\Phi\{CO_2\}$	$\Phi\{CH_3OH\}$	$\Phi\{CH_3CO_3H\}$
				$[CH_3CHO]/[O_2] = 0.32$			
41.85	10.05	31.8	0.316	0.476 (0.558)	0.171 (0.320)	0.763 (0.611)	0.562 (0.567)
259	10.0	31.4	0.318	0.270 (0.285)	0.176 (0.212)	0.547 (0.363)	0.522 (0.444)
395	10.25	31.9	0.321	0.223 (0.219)	0.171 (0.187)	0.439 (0.304)	0.378 (0.425)
635	10.2	31.6	0.323	0.151 (0.157)	0.123 (0.162)	0.316 (0.246)	0.369 (0.393)
				$[CH_3CHO]/[O_2] = 1.0$			
20.0	10.0	10.0	1.0	0.542 (0.572)	— (0.453)	1.00 (0.792)	0.929 (0.721)
201	10.1	10.1	1.0	0.313 (0.313)	0.194 (0.315)	0.708 (0.505)	0.668 (0.584)
288	10.1	10.1	1.0	0.267 (0.258)	0.259 (0.283)	0.631 (0.442)	0.658 (0.550)
425	10.2	10.1	1.0	0.194 (0.203)	0.234 (0.252)	0.462 (0.378)	0.464 (0.520)
640	10.1	9.3	1.1	0.135 (0.150)	0.204 (0.227)	0.361 (0.322)	0.510 (0.490)

[a] $I_a = 6.25 \times 10^{-4}$ Torr/s. Values of quantum yields in parentheses are computed from the mechanism and the rate coefficient ratios listed in Table 5.

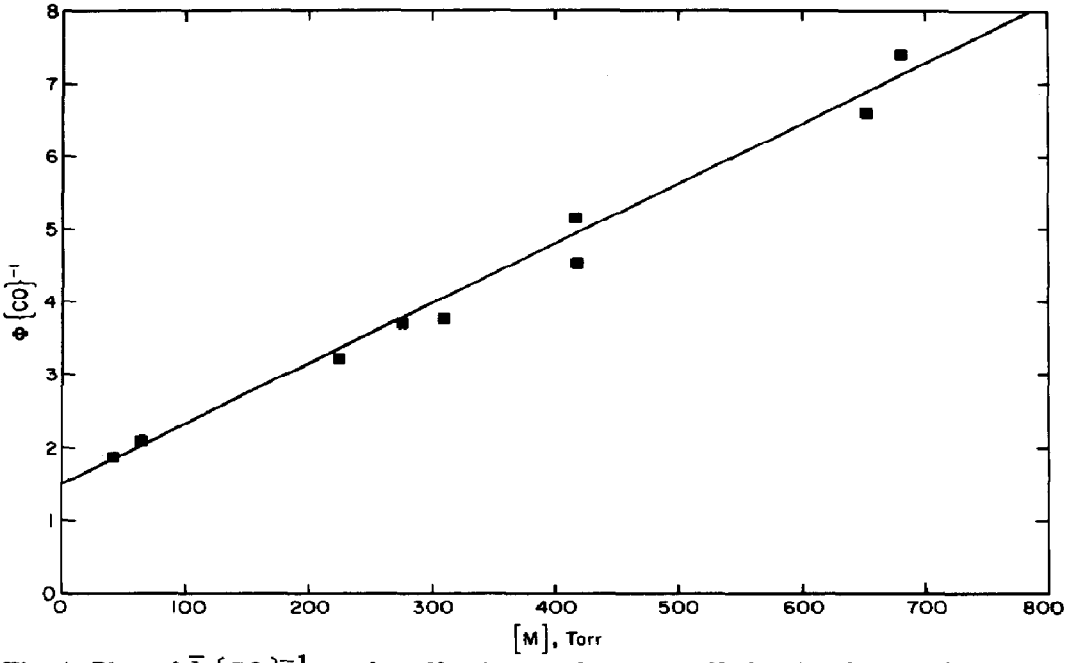

Fig. 1. Plot of $\bar{\Phi}\{CO\}^{-1}$ *vs.* the effective total pressure $[M] = [N_2] + [O_2] + 3[CH_3CHO]$ for the data in Table 2.

yields (CO, CO_2 and CH_3OH) is of the same order of magnitude as the trends in their variation with I_a, and thus there is little or no intensity dependence of the quantum yields for these products.

Table 4 gives the product quantum yields for the case of constant air pressure but with the acetaldehyde pressure varying from 3 to 30 Torr. Since acetaldehyde is the light absorbing species, changing the acetaldehyde pressure at constant air pressure causes both the absorbed light intensity and the $[CH_3CHO]/[O_2]$ ratio to change. Thus, although the quantum yields for CO_2, methanol and peracetic acid increased with increasing acetaldehyde pressure, these trends are probably due to both acetaldehyde pressure and $[CH_3CHO]/[O_2]$ ratio effects. The quantum yield of CO, however, did not change, within experimental scatter, over the range that the acetaldehyde pressure was varied indicating that $\Phi\{CO\}$ is independent of light intensity, the $[CH_3CHO]/[O_2]$ ratio, and acetaldehyde pressure.

Discussion

The primary process in CH_3CHO photolysis has been established from emission studies [17] and the triplet state induced *cis–trans* isomerization of butene-2 [18]. Parmenter and Noyes [17] found that with irradiation at 3130 Å, 16% of the excited CH_3CHO was non-quenchable, but that the remainder was quenched to the triplet state through low-lying vibrational levels of the electronically excited singlet state. Furthermore triplet CH_3CHO was not quenched by CH_3CHO. The mechanism becomes:

TABLE 3

Product quantum yields in the photolysis of acetaldehyde in the presence of air at 25 °C.
Intensity study[a]

$I_a \times 10^4$ (Torr/s)	$[CH_3CHO]$ (Torr)	[Air] (Torr)	$\Phi\{CO\}$	$\Phi\{CO_2\}$	$\Phi\{CH_3OH\}$	$\Phi\{CH_3CO_3H\}$
2.211	30.0	640	0.08 (0.158)	0.115 (0.139)	0.24 (0.218)	1.51 (1.50)
4.845	30.0	640	0.065 (0.158)	0.11 (0.139)	0.20 (0.218)	0.83 (1.03)
16.5	30.0	634	0.104 (0.159)	0.126 (0.140)	0.26 (0.219)	0.59 (0.590)
18.75	30.0	640	0.13 (0.158)	0.165 (0.139)	0.32 (0.218)	0.62 (0.555)
28.38	30.0	640	0.125 (0.158)	0.17 (0.139)	0.36 (0.218)	0.576 (0.463)

[a]Values of quantum yields in parentheses are computed from the mechanism and the rate coefficient ratios listed in Table 5.

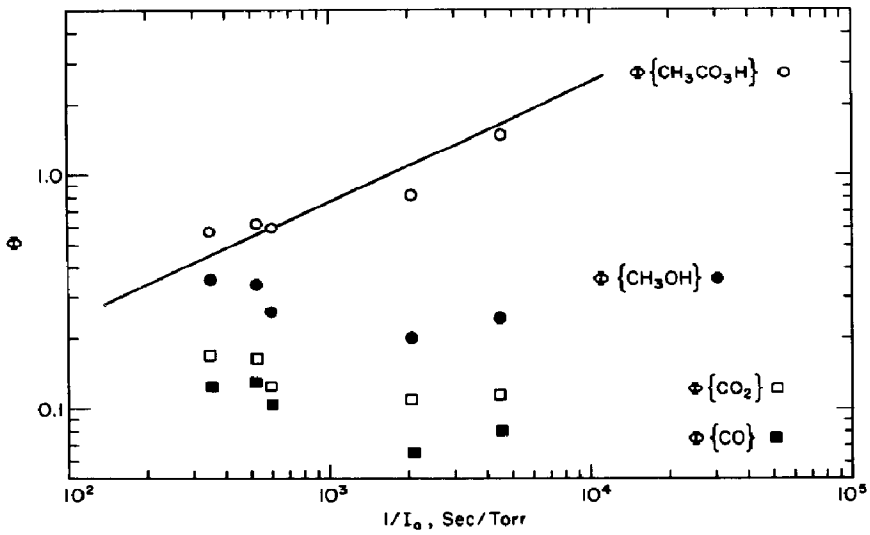

Fig. 2. Log–log plot of product quantum yields *vs.* $1/I_a$ for the data in Table 3.

$$A + h\nu \rightarrow {}^1A_n \quad (1a)$$

$$\rightarrow {}^1A' \quad (1b)$$

$${}^1A' \rightarrow CH_3 + HCO \quad (2a)$$

$$\rightarrow A \quad (2b)$$

$${}^1A_n + M \rightarrow {}^1A_0 + M \quad (3)$$

$${}^1A_0 \rightarrow {}^3A \quad (4)$$

where A is CH_3CHO, ${}^1A_n$ is the quenchable part of the electronically and vibrationally excited singlet state, ${}^1A'$ is the non-quenchable part of the electronically excited singlet state, ${}^1A_0$ is the vibrationally equilibrated electronically excited singlet state, and ${}^3A$ is the triplet state of CH_3CHO. At 3130 Å there was no CH_4 produced in the presence of NO, so that the molecular decomposition path is negligible, a result confirmed in our work here in the presence of O_2. At 3130 Å Parmenter and Noyes [17] found reactions (1a) and (1b) to proceed with efficiencies of 0.84 and 0.16, respectively.

Parmenter and Noyes [17] assumed that all the ${}^1A'$ was removed via reaction (2a), but the butene-2 quenching experiments of Archer *et al.* [18], also working with 3130 Å radiation, showed high-pressure limiting values for $\Phi\{CO\}$ and $\Phi\{CH_4\}$ to be 0.05; thus $k_{2a}/k_2 = 0.05/0.16$. In addition the work of Archer *et al.* [18] showed that ${}^3A$ was produced with a quantum efficiency between 0.79 and 0.85 in conformance with the conclusions from the emission experiments [17].

Triplet CH_3CHO is efficiently scavenged by even 1 Torr of O_2 [17] and must lead to the precursor to CO formation, since there is no other source of CO in this system except for the very minor amount from HCO oxidation. Furthermore CO production follows Stern–Volmer quenching as shown in Fig. 1. Thus the oxidation of triplet CH_3CHO proceeds via:

TABLE 4

Product quantum yields in the photolysis of acetaldehyde in the presence of air at 25 °C. $[CH_3CHO]$ study[a]

$[CH_3CHO]$ (Torr)	[Air] (Torr)	$I_a \times 10^4$ (Torr/sec)	$\Phi\{CO\}$	$\Phi\{CO_2\}$	$\Phi\{CH_3OH\}$	$\Phi\{CH_3CO_3H\}$
3.06	652	1.91	0.159 (0.173)	0.03 (0.044)	0.05 (0.088)	0.06 (0.089)
5.0	655	3.12	— (0.171)	— (0.055)	0.16 (0.105)	0.19 (0.128)
5.7	654	3.56	0.178 (0.171)	0.08 (0.059)	0.19 (0.111)	0.19 (0.141)
7.4	661	4.62	0.167 (0.168)	0.07 (0.067)	0.19 (0.122)	0.15 (0.174)
10.0	650	6.18	0.140 (0.169)	0.09 (0.080)	0.27 (0.141)	0.26 (0.227)
15.0	650	9.38	0.156 (0.166)	0.14 (0.099)	0.32 (0.167)	0.38 (0.316)
20.0	645	12.53	0.143 (0.163)	0.14 (0.115)	0.32 (0.188)	0.42 (0.401)
25.0	640	15.62	0.145 (0.161)	0.17 (0.128)	0.40 (0.205)	0.56 (0.482)
30.0	640	18.75	0.130 (0.158)	0.17 (0.139)	0.33 (0.218)	0.62 (0.463)

[a] Values of quantum yields in parentheses are calculated from the mechanism and the rate coefficient ratios listed in Table 5.

$$^3A + O_2 \rightarrow I \quad (5a)$$

$$\rightarrow A + O_2 \quad (5b)$$

$$I \rightarrow CH_3 + CO + HO_2 \quad (6)$$

$$I + M \rightarrow A + O_2 + M \quad (7)$$

where I is the intermediate to CO formation. At first thought, one might identify I as vibrationally excited CH_3CO ($+HO_2$) which could decompose to CH_3 + CO if not deactivated by collision. However, if this were the case, then CH_3CO would become increasingly important and $\Phi\{CO_2\}$ should rise to a large value as the pressure increased, contrary to the observations. Thus I must be some CH_3CHO–O_2 complex which can be deactivated to give A + O_2 or non-observed products. From Fig. 1, $k_{1a}k_{5a}/k_1k_5 = 0.65$ and $k_6/k_7 = 186$ Torr can be deduced from the intercept and slope respectively, once the very minor correction to $\Phi\{CO\}$ from HCO oxidation is made. Further fitting of the CO quantum yields, $\Phi\{CO\}$, in Table 1 at high O_2 pressure shows that O_2 is a less efficient quencher than N_2; the best fit occurs with an O_2 efficiency $\alpha\{O_2\} = 0.2$ compared to that for N_2.

The free radical processes for CH_3 and CH_3CO oxidation have been worked out in our laboratory previously [11, 19]:

$$CH_3 + O_2 \rightarrow CH_3O_2 \quad (8)$$

$$2CH_3O_2 \rightarrow 2CH_3O + O_2 \quad (9a)$$

$$\rightarrow CH_3OH + CH_2O + O_2 \quad (9b)$$

$$\rightarrow (CH_3O)_2 + O_2 \quad (9c)$$

$$CH_3CO + O_2 \rightarrow CH_3CO_3 \quad (10)$$

$$2CH_3CO_3 \rightarrow 2CH_3CO_2 + O_2 \quad (11)$$

$$CH_3O_2 + CH_3CO_3 \rightarrow CH_3O + CH_3CO_2 + O_2 \quad (12)$$

$$CH_3CO_2 \rightarrow CH_3 + CO_2 \quad (13)$$

$$CH_3O + CH_3CHO \rightarrow CH_3OH + CH_3CO \quad (14)$$

$$CH_3O + O_2 \rightarrow CH_2O + HO_2 \quad (15)$$

$$CH_3CO_3 + CH_3CHO \rightarrow CH_3CO_3H + CH_3CO \quad (16)$$

The pertinent rate coefficient ratios are listed in Table 5. Only an estimate for k_{14}/k_{15} between 10 and 20 was obtained previously (11) and we adopt the average value of 15.

The HCO oxidation has also been worked out in our laboratory. The mechanism is:

$$HCO + O_2 \rightleftharpoons HCO_3^* \quad (17a)$$

$$\rightarrow HO_2 + CO \quad (17b)$$

$$HCO_3^* + M \rightarrow HCO_3 + M \quad (18)$$

with $k_{17a}/k_{17b} = 5$ [20] and the half-quenching pressure for HCO_3^* being ~63 Torr of O_2 [21]. We assume [M] = [O_2] + [N_2] + 3[CH_3CHO], though the efficiency for N_2 is immaterial since when N_2 is added there is always sufficient pressure to make quenching complete.

TABLE 5

Rate coefficient ratios.

Ratio	Value	Units	Source
k_{1a}/k_1	0.84	None	Parmenter and Noyes [17]; Archer *et al.* [18]
k_{1b}/k_1	0.16	None	Parmenter and Noyes [17]
$k_{1b}k_{2a}/k_1k_2$	0.05	None	Archer *et al.* [18]
k_{5a}/k_5	0.77	None	Fig. 1
k_6/k_7	186	Torr	Fig. 1
$\alpha\{O_2\}/\alpha\{N_2\}$[a]	0.2	in reaction (7)	Table 1
$\alpha\{O_2\}/\alpha\{N_2\}$[a]	1.0	in reaction (18)	Assumed
$\alpha\{CH_3CHO\}/\alpha\{N_2\}$[a]	3	None	Assumed
k_{9a}/k_9	0.43	None	Weaver *et al.* [11, 19]
k_{9b}/k_9	0.50	None	Weaver *et al.* [11, 19]
k_{9c}/k_9	0.07	None	Weaver *et al.* [11, 19]
$k_{12}/(k_9k_{11})^{1/2}$	2.8	None	Weaver *et al.* [11]
k_{14}/k_{15}	15	None	Weaver *et al.* [11]
$k_{16}/k_{11}^{1/2}$	6.0×10^{-3}	$(\text{Torr sec})^{-1/2}$	Weaver *et al.* [11]
k_{17a}/k_{17b}	5	None	Osif and Heicklen [20]
k_{-17a}/k_{18}	~63	Torr	Osif [21]
$k_{23}/(k_{11}k_{22})^{1/2}$	2.0	None	Assumed
$k_{24}/(k_9k_{22})^{1/2}$	negligible	None	Assumed

α is the chaperone efficiency.

It is still necessary to decide on the fate of HCO_3. If it behaves like CH_3CO_3 then most of the time it will react with CH_3CHO:

$$HCO_3 + CH_3CHO \rightarrow HCO_3H + CH_3CO \quad (19)$$

If HCO_3 reacts with any other RO_2 (CH_3O_2, CH_3CO_3, HCO_3, but not HO_2), CH_3CO will still be produced via:

$$HCO_3 + RO_2 \rightarrow HCO_2 + RO + O_2 \quad (20)$$

$$HCO_2 + CH_3CHO \rightarrow HCOOH + CH_3CO \quad (21)$$

Thus almost all the time HCO_3 produces CH_3CO. For simplicity we assume the sole fate of HCO_3 is reaction (19). Since the HCO_3 production yields are small, this simplification introduces almost no error.

There are still three other reactions and two rate coefficient ratios that must be considered. The reactions are:

$$2HO_2 \rightarrow H_2O_2 + O_2 \quad (22)$$

$$CH_3CO_3 + HO_2 \rightarrow CH_3CO_3H + O_2 \quad (23)$$

$$CH_3O_2 + HO_2 \rightarrow CH_3O_2H + O_2 \quad (24)$$

There is no known measurement of k_{23}, so we assume $k_{23}/(k_{11}k_{22})^{1/2}$ is the statistical value of 2.0. The ratio $k_{24}/(k_9k_{22})^{1/2}$ should be similar. However, we cannot fit the data, particularly for $\Phi\{CH_3OH\}$, if reaction (24) plays any significant role, so for calculational purposes we have arbitrarily (and unjustifiably) omitted reaction (24).

With the above mechanism and the rate coefficient ratios listed in Table 5, all the quantum yields have been computed and they are listed in Tables 1 - 4 next to the observed values. For $\Phi\{CO\}$, $\Phi\{CO_2\}$, and $\Phi\{CH_3CO_3H\}$, the fits are generally within the experimental uncertainty (about ±20%). However, for $\Phi\{CH_3OH\}$, the computed values, while giving the proper trends, are almost always too low by 20 - 30%. This is in spite of the fact that we neglected reaction (24) to boost the computed values for $\Phi\{CH_3OH\}$. Either our experimental data are systematically high for some unknown reason, or there must be another process, not accounted for in the mechanism, which gives additional CH_3OH, but not CO_2. However, it is difficult to envisage what this process could be.

Application to the atmosphere

A problem of great practical importance is the rate of radical production in urban atmospheres during CH_3CHO photo-oxidation. The rate coefficient for each of the primary processes is given by:

$$k \equiv \int_{\text{all } \lambda} I_0 \epsilon \Phi \{X\} d\lambda$$

where I_0 is the incident photon flux at any wavelength λ, ϵ is the extinction coefficient (to base e) at that wavelength, and $\Phi\{X\}$ is the primary process quantum yield at that wavelength.

From the data in the literature, the quantum yields of the various primary processes can be estimated at several wavelengths, and they are given in Table 6 and plotted in Fig. 3. By drawing smooth curves through the data points, we estimate the primary quantum yields at all wavelengths. The average values $\bar{\phi}$ for 50 Å intervals are listed in Table 7 along with the incident photon fluxes for 50 Å intervals at the surface of the earth for an overhead sun. (For $\bar{\phi}\{CO + CH_3 + HO_2\}$ we take 18% of $\phi\{\text{triplet}\}$ as found here at 3130 Å. We have measured the extinction coefficients for CH_3CHO, and the 50 Å average values $\bar{\epsilon}$ are also listed in Table 7. The product $I_0 \bar{\epsilon} \bar{\phi} \{X\}$ gives the rate coefficient for each process for the 50 Å interval, and the sum of these products gives the overall rate coefficient at the earth's surface for an overhead sun. The values are:

k (s^{-1})	process
4.1×10^{-7}	$CH_4 + CO$
2.8×10^{-6}	$CH_3 + HCO$
8.7×10^{-6}	$CH_3 + CO + HO_2$

The overall rate coefficient for the production of all free radicals is 2.3×10^{-5} s^{-1}.

TABLE 6

Quantum yields of the primary processes in acetaldehyde photo-oxidation as a function of excitation wavelength.

λ (Å)	$\phi\{CO + CH_4\}$	$\phi\{CH_3 + HCO\}$	$\phi\{\text{Triplet}\}$
3340	0	0	1.0[d]
3130	0	0.05[b]	0.84[e]
2967	—	—	0.59[d]
2804	0.15[a]	≲0.30[c]	0.48[d]
2654	0.28[a]	0.36[a]	—
2537	0.64[a]	0.36[a]	—

[a]From Calvert and Pitts [22].
[b]This work and Archer *et al.* [18].
[c]Calculated from the total quantum yield of the free radical processes ($\phi\{CH_3 + HCO\} = 0.39$, Calvert and Pitts [22]); the fraction of that from the triplet, 0.18; and $\phi\{\text{triplet}\}$ at 2804 Å = 0.48.
[d]From Parmenter and Noyes [17].
[e]From Parmenter and Noyes [17] and Archer *et al.* [18].

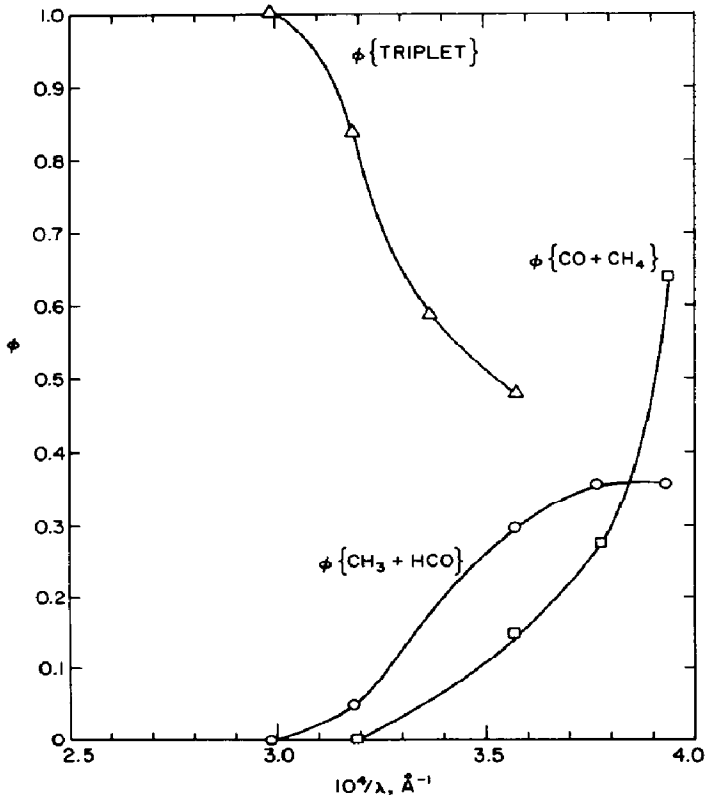

Fig. 3. Quantum yields for the various primary processes in CH_3CHO photolysis *vs.* the reciprocal excitation wavelength.

TABLE 7

Photodissociation rate coefficients for acetaldehyde.

λ (Å)	$\bar{\epsilon}$[a] (cm^2 molec.$^{-1}$)	I_a[b] (photons per cm^2 sec 50 Å)	$CH_4 + CO$		$CH_3 + HCO$		$CO + CH_3 + HO_2$	
			$\bar{\phi}$	$\bar{\phi}\bar{\epsilon}I_0$ (s^{-1}/50 Å)	$\bar{\phi}$	$\bar{\phi}\bar{\epsilon}I_0$ (s^{-1}/50 Å)	$\bar{\phi}$	$\bar{\phi}\bar{\epsilon}I_0$ (s^{-1}/50 Å)
2900 - 2950	4.62×10^{-20}	3×10^{12}	0.075	1.04×10^{-8}	0.212	2.94×10^{-8}	0.100	1.39×10^{-8}
2950 - 3000	4.28×10^{-20}	2×10^{13}	0.055	4.71×10^{-8}	0.172	1.47×10^{-7}	0.108	9.24×10^{-8}
3000 - 3050	3.77×10^{-20}	1.3×10^{14}	0.035	1.71×10^{-7}	0.132	6.47×10^{-7}	0.116	5.69×10^{-7}
3050 - 3100	3.06×10^{-20}	2.5×10^{14}	0.018	1.38×10^{-7}	0.095	7.27×10^{-7}	0.128	9.79×10^{-7}
3100 - 3150	2.37×10^{-20}	4×10^{14}	0.005	4.74×10^{-8}	0.060	5.69×10^{-7}	0.145	1.37×10^{-6}
3150 - 3200	1.81×10^{-20}	5.1×10^{14}	0	0	0.038	3.5×10^{-7}	0.161	1.49×10^{-6}
3200 - 3250	1.38×10^{-20}	6.25×10^{14}	0	0	0.025	2.1×10^{-7}	0.169	1.45×10^{-6}
3250 - 3300	8.80×10^{-21}	7.5×10^{14}	0	0	0.012	7.9×10^{-8}	0.175	1.15×10^{-6}
3300 - 3350	4.79×10^{-21}	9×10^{14}	0	0	0.002	8.6×10^{-9}	0.178	7.67×10^{-7}
3350 - 3400	2.85×10^{-21}	9.5×10^{14}	0	0	0	0	0.179	4.84×10^{-7}
3400 - 3450	1.54×10^{-21}	1.0×10^{15}	0	0	0	0	0.179	2.76×10^{-7}
3450 - 3500	3.87×10^{-22}	1.05×10^{15}	0	0	0	0	0.179	7.27×10^{-8}
3500 - 3550	0	1.1×10^{15}	—	—	—	—	—	—
Total (s^{-1})				4.14×10^{-7}		2.77×10^{-6}		8.71×10^{-6}

[a]This work.
[b]From Heicklen [23].

Acknowledgements

This work was supported by the Environmental Protection Agency through Grant No. 800874 and the Center for Air Environment Studies at the Pennsylvania State University (C.A.E.S. Report No. 422-76) for which we are grateful.

References

1 S. L. Kopczynski, A. P. Altshuller and F. D. Sutterfield, Env. Sci. Technol., 8 (1974) 909.
2 A. P. Altshuller, D. L. Klosterman, P. W. Leach, I. J. Hindawi and J. E. Sigsby, Jr., Int. J. Air Water Pollut., 10 (1966) 81.
3 E. J. Bowen and E. L. Tietz, J. Chem. Soc., (1930) 234.
4 J. E. Carruthers and R. G. W. Norrish, J. Chem. Soc., (1936) 1036.
5 J. Mignolet, Bull. Soc. R. Sci. Liège, 10 (1941) 343.
6 C. A. McDowell and L. K. Sharples, Can. J. Chem., 36 (1958) 251.
7 C. A. McDowell and L. K. Sharples, Can. J. Chem., 36 (1958) 268.
8 C. A. McDowell and S. Sifoniades, Can. J. Chem., 41 (1963) 300.
9 J. G. Calvert and P. L. Hanst, Can. J. Chem., 37 (1959) 1671.
10 H. S. Johnston and J. Heicklen, J. Am. Chem. Soc., 86 (1964) 4254.
11 J. Weaver, J. Meagher, R. Shortridge and J. Heicklen, J. Photochem., 4 (1975) 341.
12 N. A. Clinton, R. A. Kenley and T. G. Traylor, J. Am. Chem. Soc., 97 (1975) 3746.
13 P. A. Giguere and A. W. Olmos, Can. J. Chem., 30 (1952) 821.
14 F. H. MacDougall, J. Am. Chem. Soc., 58 (1936) 2585.
15 R. Renaud and L. C. Leitch, Can. J. Chem., 32 (1954) 549.
16 S. C. Chan, B. S. Rabinovitch, J. T. Bryant, L. D. Spicer, T. Fujimoto, Y. N. Lin and S. P. Pavlou, J. Phys. Chem., 74 (1970) 3160.
17 C. S. Parmenter and W. A. Noyes, Jr., J. Am. Chem. Soc., 85 (1963) 4161.
18 A. S. Archer, R. B. Cundall and T. F. Palmer, Proc. R. Soc., A334 (1973) 411.
19 J. Weaver, R. Shortridge, J. Meagher and J. Heicklen, J. Photochem., 4 (1975) 109.
20 T. Osif and J. Heicklen, unpublished work (1975).
21 T. Osif, unpublished work (1975).
22 J. G. Calvert and J. N. Pitts, Jr., Photochemistry, Wiley, New York, (1966) p. 371.
23 J. Heicklen, Atmospheric Chemistry, Academic Press, London.